Original Article

Feasibility of magnetization-transfer-contrast relaxation-enhanced angiography without contrast and triggering (REACT) imaging at 1.5 T combined with deep learning-based reconstruction for cardiovascular visualization

Sukran Erdem[1], Alexandra Jack[2], Pezad Doctor[1], Gerald Greil[1,3,4], Tarique Hussain[1,3,4], Qing Zou[1,3,4]

[1]Division of Cardiology, Department of Pediatrics, University of Texas Southwestern Medical Center, Dallas, TX, USA; [2]Department of Biomedical Engineering, University of Michigan, Ann Arbor, MI, USA; [3]Department of Radiology, University of Texas Southwestern Medical Center, Dallas, TX, USA; [4]Advanced Imaging Research Center, University of Texas Southwestern Medical Center, Dallas, TX, USA

Contributions: (I) Conception and design: T Hussain, Q Zou; (II) Administrative support: T Hussain, G Greil, Q Zou; (III) Provision of study materials or patients: Q Zou; (IV) Collection and assembly of data: S Erdem, A Jack, Q Zou; (V) Data analysis and interpretation: S Erdem, A Jack; (VI) Manuscript writing: All authors; (VII) Final approval of manuscript: All authors.

Correspondence to: Qing Zou, PhD. Division of Cardiology, Department of Pediatrics, University of Texas Southwestern Medical Center, 5323 Harry Hines Boulevard, Dallas, TX 75390, USA; Department of Radiology, University of Texas Southwestern Medical Center, Dallas, TX, USA; Advanced Imaging Research Center, University of Texas Southwestern Medical Center, Dallas, TX, USA. Email: Qing.Zou@UTSouthwestern.edu.

Background: Relaxation-enhanced angiography without contrast and triggering (REACT) is a flow-independent three-dimensional (3D) magnetic resonance angiography sequence designed to minimize artifacts using the Dixon method and an inversion recovery pre-pulse. A magnetization transfer contrast (MTC) pre-pulse (MTC-REACT) may further enhance image quality. This study evaluates the feasibility of MTC-REACT and examines deep learning-based reconstruction to improve image quality for pulmonary veins.

Methods: This study was approved by the institutional review board. Twenty participants were prospectively recruited. Ten-fold undersampling was applied for REACT and MTC-REACT data acquisition. The inline compressed sense (CS) reconstruction algorithm, and an off-line Adaptive-CS-Net algorithm, were used for MTC-REACT and REACT image reconstruction. Commercially available analysis software was used for multi-planar reformatting, signal-to-noise ratio (SNR), contrast-to-noise ratio (CNR) measurements, and image quality analysis. Categorical data were compared with a Wilcoxon signed ranks test and normally distributed variables with a *t*-test.

Results: The Adaptive CS-Net reconstructed MTC-REACT images provided significantly higher SNR and CNR for right pulmonary veins (SNR 33.9±4.1, 30.3±3.4; CNR 33.3±3.4, 29.6±4.3), and left pulmonary veins (SNR 35.0±3.6, 31.2±4.3; CNR 34.6±4.2, 30.6±4.4) with all P values <0.05 compared to the CS-reconstructed MTC-REACT sequence. When Adaptive CS-Net reconstruction is used for both techniques, MTC-REACT images displayed significantly higher SNR and CNR compared to the REACT sequence for only left pulmonary veins (SNR 35±3.3, 32.4±4.6; CNR 34.6±3.4, 31.8±4.6). The Adaptive-CS-Net reconstructed MTC-REACT sequence consistently outperforms the CS-reconstructed MTC-REACT for pulmonary artery and vein imaging.

Conclusions: The Adaptive-CS-Net reconstructed MTC-REACT images consistently deliver superior CNR, and SNR compared to the CS reconstructed images for pulmonary veins. Notably, the MTC-REACT technique enhances image quality for pulmonary veins compared to the REACT sequence, irrespective of the deep-learning reconstruction method's impact.

Keywords: Magnetization transfer contrast (MTC); relaxation-enhanced angiography without contrast and triggering (REACT); whole-heart magnetic resonance imaging (WH MRI); pulmonary veins

Submitted Oct 11, 2024. Accepted for publication Feb 18, 2025. Published online Mar 28, 2025.
doi: 10.21037/qims-24-2199
View this article at: https://dx.doi.org/10.21037/qims-24-2199

Introduction

Three-dimensional (3D) whole-heart (WH) imaging, utilizing contrast-enhanced balanced steady-state free precession (bSSFP) sequence, is a widely used cardiovascular magnetic resonance (CMR) imaging technique. This method generates detailed 3D images of the heart and great vessels within the thorax, making it a standard tool for anatomical evaluation for patients with both congenital and acquired heart diseases (1-3). Despite its utility, 3D bSSFP imaging is highly susceptible to off-resonance effects, often resulting in reduced image quality due to banding artifacts, signal loss, or inadequate fat suppression (4). In non-contrast 3D bSSFP acquisitions, signal voids are frequently observed in regions such as pulmonary veins and the left atrium (5-7). Contrast-enhanced 3D WH imaging, despite its better performance, also has inherent risks associated with using contrast media (8). As an alternative, several non-contrast-enhanced 3D WH imaging techniques have been developed. However, these approaches face significant limitations, including lower spatial resolution, reduced contrast-to-noise ratio (CNR), and diminished signal-to-noise ratio (SNR). These challenges can complicate the visualization of cardiovascular structures, potentially limiting their clinical application (9-12).

A recently introduced magnetic resonance angiography (MRA) method—relaxation-enhanced angiography without contrast and triggering (REACT)—has demonstrated promising results for angiographic imaging of vascular structures outside the heart (13,14). Its application has since been expanded to venography in the pelvis and low extremities (15) as well as to non-contrast-enhanced 3D WH imaging through the integration of motion correction techniques such as electrocardiogram (ECG) triggering and respiratory-triggering (16,17). This method shows significant potential for the clinical assessment of cardiac and thoracic vascular anatomy in pediatric and adult populations with complex congenital heart disease (CHD) and vasculopathy.

REACT employs the dual-echo Dixon technique, a chemical shift-encoded fat-water separation method, for uniform suppression of background tissue across the field of view, using a non-balanced gradient echo readout (14). This approach provides robust fat suppression over large fields of view, such as the subclavian area. Furthermore, this technique demonstrates enhanced resilience to magnetic field inhomogeneities, which are particularly common in the thoracic cavity (18). Moreover, in a recent study, REACT performance was compared to a non-contrast-enhanced 3D bSSFP sequence at 1.5 Tesla (T), and the REACT technique was found to provide superior image quality for subclavian veins (19).

Magnetization transfer contrast (MTC) pulses have also been proposed as useful adjuncts to MRA techniques. MTC preparation provides more resistance to flow-mediated off-resonance effects than standard T2 preparation pulses, leading to improved imaging of pulmonary veins (2). This study investigates whether combining MTC pre-pulse with the REACT sequence might enhance image quality and reduce artifacts in extracardiac great vessels compared to conventional REACT sequences.

In current clinical settings, the images acquired with the REACT sequence are commonly reconstructed with parallel imaging or more frequently with compressed sense (CS) (17-21). But for the desired higher undersampling factors to get faster image acquisition, CS's performance is limited to the choice of the sparsity representation and the tuning of the corresponding reconstruction parameters (22). Deep learning (DL)-based reconstruction algorithms have recently been proposed to solve these problems efficiently. Using high undersampling factors reduces the amount of acquired data, shortens scanning times, and minimizes the likelihood of bulk motion artifacts (23).

This study explores the potential to enhance image quality and reduce acquisition times for MTC-REACT by employing highly undersampled data (10-fold undersampling) and a DL-based magnetic resonance imaging (MRI) reconstruction framework. Quantitative and qualitative comparisons were conducted between the CS-reconstructed MTC-REACT and Adaptive-CS-Net-

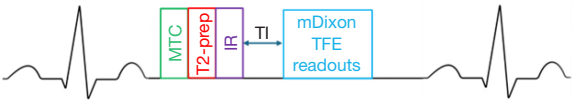

Figure 1 Visual illustration of the MTC-REACT sequence. Before the mDixon turbo field echo readouts, three prepulses were performed, including MTC, T2-prep, and IR. IR, inversion recovery; mDixon, modified Dixon; MTC, magnetization transfer contrast; REACT, relaxation-enhanced angiography without contrast and triggering; T2 prep, T2 preparation; TFE, turbo field echo; TI, inversion time.

reconstructed MTC-REACT images to assess the utility of DL-based reconstruction. Additionally, image quality was evaluated through qualitative and quantitative comparisons of the Adaptive-CS-Net-reconstructed MTC-REACT and REACT sequences, highlighting the contribution of the MTC pre-pulse to image quality. Furthermore, this study provides detailed insights into important sequence parameters for the MTC-REACT technique. We present this article in accordance with the TRIPOD + AI reporting checklist (available at https://qims.amegroups.com/article/view/10.21037/qims-24-2199/rc).

Methods

The study was conducted in accordance with the Declaration of Helsinki (as revised in 2013). The study was approved by the local institutional review board of the University of Texas Southwestern Medical Center (No. STU 032016009), and informed consent was obtained from all individual participants. Twenty subjects undergoing CMR imaging for clinical purposes or volunteering for this research study were recruited between April and August 2024.

MRI protocol

All data were acquired using a 1.5 T clinical MR scanner (Ingenia Philips Healthcare, Best, The Netherlands) with a 32-array receiver torso coil. All 3D acquisitions were performed in the transverse plane. The MTC-REACT and REACT images were acquired at the mid-diastolic phase. The sequence parameters of the REACT and MTC-REACT are as follows: time to first echo (TE1)/time to second echo (TE2)/time to repetition (TR) =1.88/4.5/6.8 milliseconds (ms), flip angle =15°, acquired isotropic voxel size 1.6 cubic millimeters (mm^3), reconstruction isotropic voxel size 0.8 mm^3, undersampling factor =10. The TE1 and TE2 values were automatically determined by the scanner and represent the minimal echo times achievable for the system. The raw k-space data were saved for the REACT and MTC-REACT sequences for off-line deep-learning-based reconstruction for comparison. Other than these research sequences in the whole imaging protocol for healthy volunteers, other sequences in the protocol include the two-dimensional (2D) bSSFP images for cardiac cine, 2D phase-contrast images for flow measurements as well as the late gadolinium enhancement imaging. The total time for the whole protocol is about 1.5 hours. For patients with CHD, the complete imaging protocol includes cardiac cine, flow, and contrast-enhanced 3D bSSFP imaging other than the research sequences. The sequence parameters for contrast-enhanced 3D bSSFP sequence include: TE/TR =2.0/4.0 ms, flip angle =90°, acquired voxel size =1.2 mm × 1.2 mm × 1.8 mm (foot-head × right-left × anteroposterior) and reconstructed voxel size =0.98 mm × 0.98 mm × 0.9 mm. SENSitivity Encoding (SENSE) acceleration factor of 1.5 on both right-left and snteroposterior direction is used for speeding up the 3D bSSFP acquisition. The total time for the whole protocol is about 1 hour. For all the studies, gadolinium contrast (Gadavist®, Bayer HealthCare LLC, NJ, USA) with dosage of 1 mL/kg was used.

MTC-REACT sequence description

For data acquisition, we used respiratory navigation and ECG triggering combined with a 3D magnetization prepared non-balanced dual-echo Dixon technique, which was first proposed by Yoneyama *et al.* (14). The original REACT sequence starts with a set of magnetization preparations, which consists of a four adiabatic-based T2-preparation module. Then, a non-volume-select short tau inversion recovery (STIR) pre-pulse with a short inversion recovery time (TI) occurs (13). In this work, a magnetization transfer (MT) on-resonance pre-pulse, as proposed in (24), is added before the T2 pre-pulse to enhance tissue contrast between vessels and background tissues as illustrated in *Figure 1*. MTC accounts for the continuous exchange of magnetization between free-pool protons and bound-pool protons. This technique utilizes the difference in the frequencies between free-pool and bound-pool protons, with bound-pool protons having a much lower frequency, to

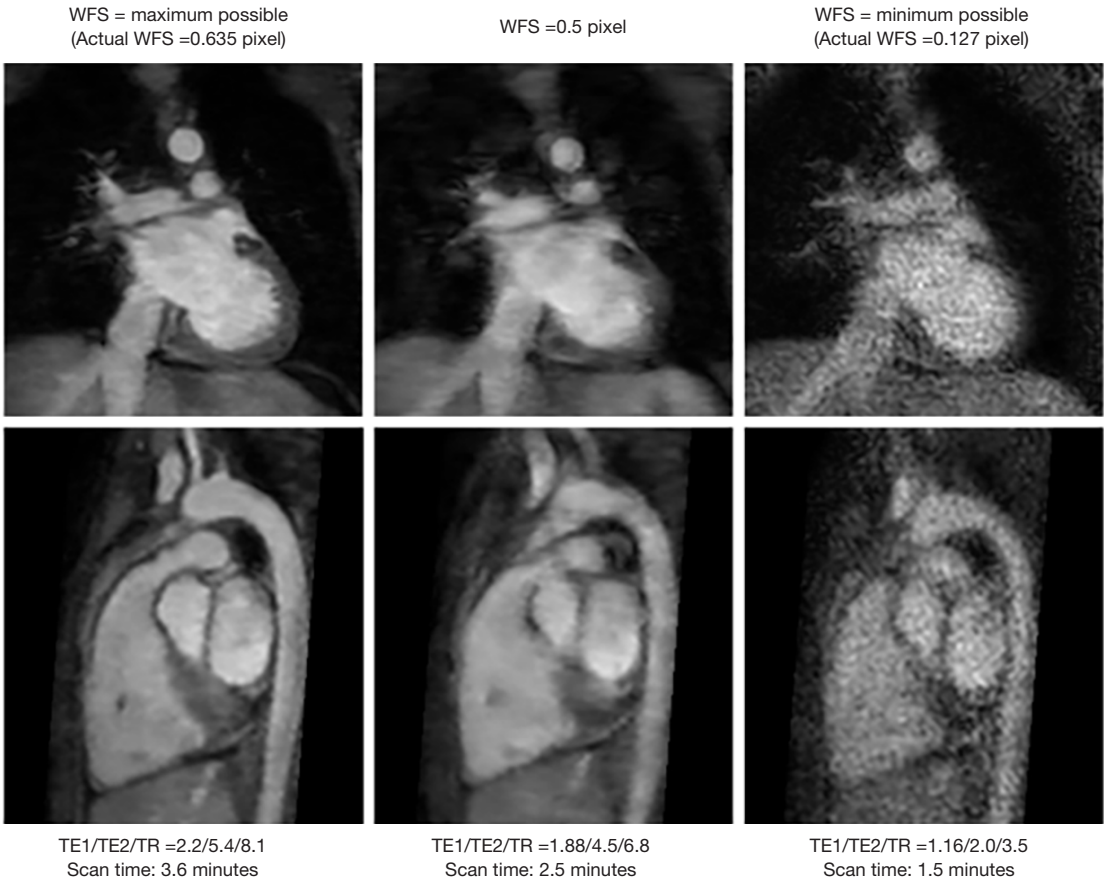

Figure 2 Impact of the WFS on image quality and scan time. MTC-REACT water-only images, in coronal (upper row) and sagittal (lower row) views from an 18-year-old, female subject are presented. When the WFS is set to its maximum possible value, the best image quality is achieved, though at the cost of the longest scan time (left column). With the WFS set to 0.5 pixels, a slight degradation in image quality is observed, including some blurring, but the scan time is reduced by 30% (middle column). When the WFS is set to the minimum possible value, the SNR is significantly reduced; however, the scan time is reduced by 59% (right column). The blood pool to background SNR/CNR =22.3/21.6, 21.1/19.8, 16.6/14.3 for the maximum possible, 0.5 pixels, and minimum possible WFS, respectively. CNR, contrast-to-noise ratio; MTC-REACT, magnetization transfer contrast-relaxation-enhanced angiography without contrast and triggering; SNR, signal-to-noise ratio; TE1, echo time 1; TE2, echo time 2; TR, time to repetition; WFS, water-fat shift.

design an MTC pre-pulse. With this technique, bound-pool protons are also selectively saturated, and the background signal is suppressed, improving the visibility of vascular structures (25), such as the pulmonary veins and arteries (26). A 3D-adjusted two-point chemical-shift water-fat separation turbo field echo [modified Dixon (mDixon) turbo field echo (TFE)] pulse sequence is implemented to acquire the data. The water-fat shift (WFS) and the duration of the TFE shot were optimized for image quality and total acquisition time. Based on the studies shown in *Figures 2,3*, the WFS is chosen as 0.5 pixels and the TFE shot duration is chosen as every 2 heartbeats, and such parameters are also used for the REACT sequence. The sequence diagram of the proposed MTC-REACT can be seen in *Figure 1*. The T2-preparation time is 50 ms and the inversion delay is set as shortest (12.2 ms). The inversion delay for the original REACT sequence is 7.8 ms. The MTC pre-pulse duration is 20 ms. Regarding respiratory triggering, we employed a pencil beam navigator to reduce significant artifacts from respiratory motion. Additionally, we used ECG triggering to account for the heart's motion and obtain static cardiac images at the mid-diastolic phase.

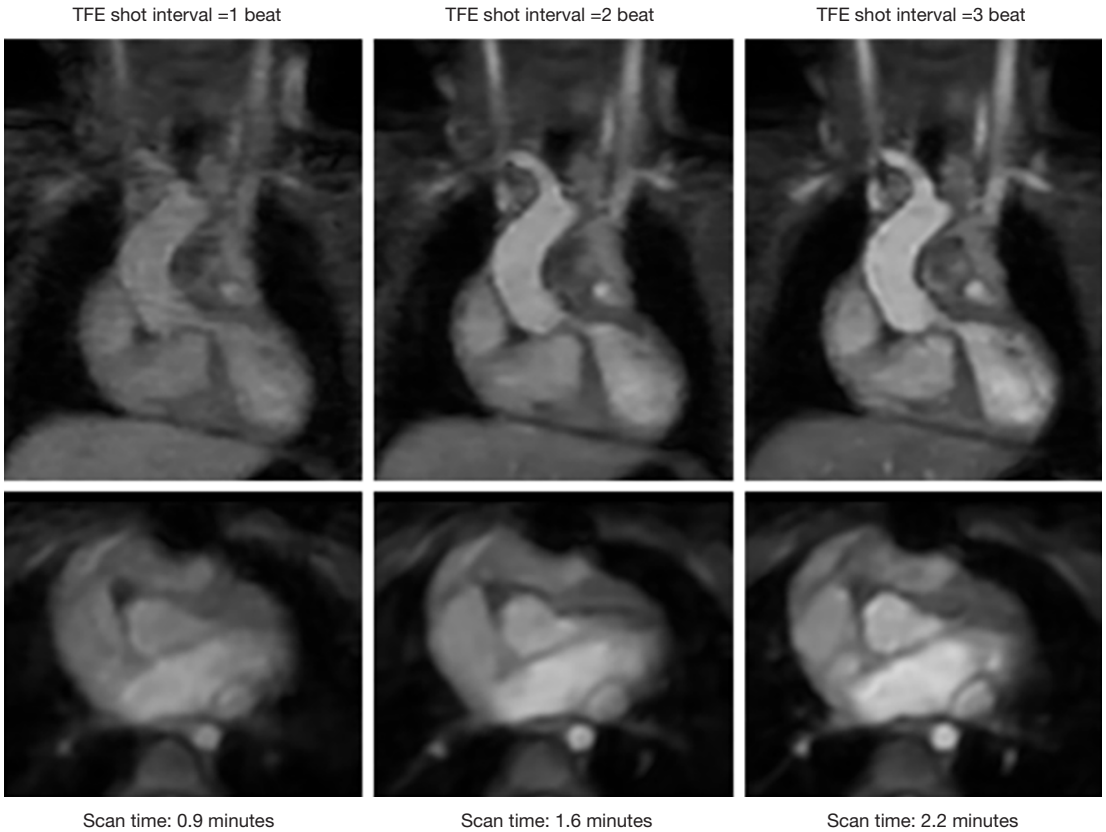

Figure 3 Impact of the TFE shot interval on image contrast and scan time. Clinical datasets with varying TFE shot intervals and the corresponding MTC-REACT images were obtained from a 2-year-old male patient with critical pulmonary valve stenosis and a perimembranous VSD, following pulmonary valvuloplasty and VSD closure. When the TFE shot interval is chosen as the minimum possible value (1 heartbeat), the scan time is the shortest, but the image contrast and image quality are the worst. When the TFE shot interval is chosen as 2 heartbeats, image quality, and image contrast have improved, but the scan time is increased by 78%. When the TFE shot interval is further increased to 3 heartbeats, slightly improved image quality can be achieved, but the scan time is increased by 38% compared to the TFE shot interval of 2 heartbeats. The blood pool to background SNR/CNR = 17.2/15.8, 20.6/18.7, 22.1/21.3 for 1 heartbeat, 2 heartbeats, and 3 heartbeats TFE shot interval, respectively. CNR, contrast-to-noise ratio; MTC-REACT, Magnetization Transfer Contrast-relaxation-enhanced angiography without contrast and triggering; TFE, turbo field echo; SNR, signal-to-noise ratio; VSD, ventricular septal defect.

Adaptive CS-Net reconstruction algorithm

For the images acquired using the REACT sequence, the in-line CS (Compressed SENSE, Philips Healthcare) reconstructions were saved for comparison, and the 10-fold undersampled raw k-space data were saved for off-line reconstruction using Adaptive CS-Net for comparison purposes.

For deep-learning-based reconstruction, the Adaptive-CS-Net (27) which is based on the iterative shrinkage-thresholding algorithm (ISTA)-Net (28) is used to get the reconstruction. The Adaptive-CS-Net was chosen in this work due to the support including training data and implementation provided by the MR vendor (Philips).

Quantitative image quality analysis

Quantitative image analysis was performed using MATLAB-MathWorks (R2022a). To accurately assess and quantify the image quality, we utilized two image quality metrics: SNR and CNR. A higher SNR value indicates a better image quality than a lower SNR. This study took SNR measurements of the heart, lung, liver, and left and right pulmonary veins. Regions of interest (ROIs) for each patient were manually selected. To compute SNR (in

decibels), the following equation was employed (29):

$$SNR = 20 \cdot \log\left(\frac{\mu}{\sigma}\right) \quad [1]$$

where log indicates the base 10 logarithmic function, μ is the mean intensity value of the ROI and σ represents the standard deviation of the noise region. Similarly, CNR (in decibels) is used to evaluate image quality, however, it measures the contrast difference between the ROI and background region, and the following equation was used (29):

$$CNR = 20 \cdot \log\left(\frac{\mu_{signal} - \mu_{background}}{\sigma_{noise}}\right) \quad [2]$$

In this equation, μ_{signal} and $\mu_{background}$ represent the mean intensity values of the ROI and background region, and σ_{noise} is the standard deviation of the noise region. In this work, we choose a region under the arm region as background ROI.

Qualitative image quality analysis

Commercially available analysis software RadiAnt Dicom Viewer (2024.1, Medixant, Poznan, Poland) was used for qualitative image quality analysis and multi-planar reformatting. Coronary artery origins, left and right pulmonary artery, right upper and lower pulmonary veins, left upper and lower pulmonary veins were analyzed for image quality. The same windowing level and matched geometry were used for fair comparison between methods. Two experienced pediatric cardiologists who are trained in advanced cardiac imaging independently conducted a blind assessment of image quality, focusing on reformatted angiograms of each area of interest, and then consensus grades were given. Image quality assessment based on a 5-point Likert scale (30) and was divided on the sharpness of vessel borders and noise levels (1= nondiagnostic, vessels are not identifiable, 2= poor image quality with severe artifacts, severe noise and vessel blurring, 3= adequate image quality for diagnosis with some vessel blurring, noise and artifacts, 4= good image quality with minimal vessel blurring, noise and artifacts, 5= excellent image quality with good vessel border delineation, no noise).

Statistical analysis

Statistical analysis was performed using commercially available software (SPSS, version 29.0.2), with statistical significance set at P<0.05. Image quality measurements, representing categorical data, were assessed using the nonparametric Kruskal-Wallis test for overall comparisons and the Wilcoxon Rank-Sum tests for pairwise comparisons between the 4 sets of images.

SNR and CNR measurements of REACT, CS reconstructed MTC-REACT, and Adaptive-CS-Net reconstructed MTC-REACT were tested for normality with the Kolmogorov-Smirnov test. After confirming normal distribution, SNR and CNR values of CS and Adaptive-CS-Net reconstructed MTC-REACT were compared using paired *t*-tests.

Results

ECG-triggered and respiratory navigator-gated REACT and MTC-REACT acquisitions and reconstructions were completed successfully in all healthy volunteers and patients with CHD (n=20, mean age: 15.8±6.55 years). The mean age was (2 females, 3 males) 12.6±8 years for patients with CHD and 16.9±5.9 years for healthy volunteers (9 females, 6 males). All participants were in sinus rhythm. Two patients (mean age: 4.5 years) underwent imaging under general anesthesia. The REACT sequence has an average acquisition time of 2.4 minutes while the MTC-REACT sequence averages 2.5 minutes. Average reconstruction times are 43 seconds for CS and 28 seconds for Adaptive-CS-Net. The heart rate for 20 subjects ranges from 62 to 100 bpm.

Quantitative image quality comparison

For the quantitative comparison of image quality between the Adaptive-CS-Net reconstructed MTC-REACT and the CS-reconstructed MTC-REACT, SNR, and CNR values for specific ROIs were analyzed and presented in *Table 1*. The Adaptive-CS-Net reconstructed MTC-REACT images demonstrated statistically significantly higher SNR values for the blood pool (20.7±3.1, 19.6±3.3), liver (12.9±2.8, 11.6±2.1), lung (19.0±2.5, 17.9±2.6), and right (33.9±4.1, 30.3±3.4) and left pulmonary veins (35.0±3.6, 31.2±4.3) compared to the CS-reconstructed MTC-REACT method with all P<0.05 (*Table 1*). Similarly, the Adaptive-CS-Net reconstructed MTC-REACT images showed statistically significant improvements in CNR compared to CS-reconstructed MTC-REACT images for blood pool (15.9±2.4, 15.0±2.6); left pulmonary vein (34.6±4.2, 30.6±4.4); right pulmonary vein (33.3±3.4, 29.6±4.3) with all P<0.05 (Adaptive-Net *vs.* CS reconstructed MTC-REACT,

Table 1 SNR and CNR comparison between MTC-REACT images reconstructed using CS and Adaptive-CS-Net

Region of interest	CS	Adaptive-CS-Net	P value
SNR			
Blood pool	19.6±3.3	20.7±3.1	**
Liver	11.6±2.1	12.9±2.8	**
Lung	17.9±2.6	19.0±2.5	**
LPV	31.2±4.3	35.0±3.6	**
RPV	30.3±3.4	33.9±4.1	**
CNR			
Blood pool	15.0±2.6	15.9±2.4	**
LPV	30.6±4.4	34.6±4.2	**
RPV	29.6±4.3	33.3±3.4	**

The values in the table are the mean ± standard deviation of all the subjects. **, the corresponding P value is less than 0.05. CNR, contrast-to-noise ratio; CS, compressed sense; LPV, left pulmonary vein; MTC-REACT, magnetization transfer contrast relaxation-enhanced angiography without contrast and triggering; RPV, right pulmonary vein; SNR, signal-to-noise ratio.

Table 2 SNR and CNR comparison between REACT and MTC-REACT

Region of interest	REACT	MTC-REACT	P value
SNR			
Blood pool	20.6±3.1	20.7±2.2	*
LPV	32.4±4.6	35.0±4.1	**
RPV	31.9±3.8	33.9±4.1	**
CNR			
Blood pool	13.7±2.1	15.9±2.6	**
LPV	31.8±4.6	34.6±3.4	**
RPV	31.2±4.3	33.3±4.5	*

The values in the table are the mean ± standard deviation of all the subjects. *, the corresponding P value is larger than 0.05; **, the corresponding P value is less than 0.05. CNR, contrast-to-noise ratio; LPV, left pulmonary vein; MTC-REACT, magnetization transfer contrast relaxation-enhanced angiography without contrast and triggering; RPV, right pulmonary vein; SNR, signal-to-noise ratio.

respectively).

Additionally, *Table 2* provides a detailed comparison of SNR and CNR values between the Adaptive-CS-Net reconstructed REACT sequence and the Adaptive-CS-Net reconstructed MTC-REACT sequences. The Adaptive-CS-Net reconstructed MTC-REACT method achieved statistically significant improvements in SNR for the left (35.0±3.3, 32.4±4.6, P<0.05) and right pulmonary veins (33.9±4.1, 31.9±3.8, P<0.05) compared to Adaptive-CS-Net reconstructed REACT sequence, while the blood pool SNR values were comparable between the two methods (20.7±2.2, 20.6±3.1, P>0.05). Furthermore, the Adaptive-CS-Net reconstructed MTC-REACT method demonstrated statistically significantly higher CNR values for the blood pool (15.9±2.6, 13.7±2.1, P<0.05) and left pulmonary veins (34.6±3.4, 31.8±4.6, P<0.05). In contrast, the right pulmonary veins (33.3±4.5, 31.2±4.3, P>0.05) showed similar CNR values between the two methods (*Table 2*).

Qualitative image quality analysis

Image quality scores comparing the performance of all methods, along with their statistical values, are presented in *Table 3*. Significant differences in image quality are observed between the MTC-REACT and REACT sequences when reconstructed with either CS or Adaptive-CS-Net, except for the left coronary artery (P=0.039 for the right coronary artery, P=0.07 for the left coronary artery).

For the right coronary artery, the Adaptive-CS-Net reconstructed MTC-REACT outperforms the CS reconstructed REACT (P=0.005). However, no significant differences are found in other pairwise comparisons for this region. For the left coronary artery, the differences are minimal, with only one pairwise comparison showing significance (Adaptive-CS-Net reconstructed REACT *vs.* CS reconstructed REACT, P=0.044).

The Adaptive-CS-Net reconstructed MTC-REACT sequence consistently outperforms both the CS-reconstructed MTC-REACT and the CS-reconstructed REACT sequences for pulmonary artery and vein imaging.

When MTC-REACT and REACT sequences are reconstructed using the same reconstruction method, whether Adaptive-CS-Net or CS, they yield similar image quality scores for all ROIs.

Visual comparison of Adaptive-CS-Net and CS-reconstructed MTC-REACT methods

All the figures presented in this paper are water-only images. The images were reformatted using the same windowing level and matched geometry to ensure a fair comparison between the sequences.

Table 3 Image quality comparison between imaging methods

	P value						
	MTC-REACT-DL *vs.* MTC-REACT-CS	MTC-REACT-DL *vs.* REACT-DL	MTC-REACT-DL *vs.* REACT-CS	MTC-REACT-CS *vs.* REACT-DL	MTC-REACT-CS *vs.* REACT-CS	REACT-DL *vs.* REACT-CS	All
Left pulmonary artery	0.0001†	0.366	0.0001†	0.0001‡	0.828	0.0001†	0.001
Right pulmonary artery	0.0001†	0.366	0.0001†	0.0001‡	0.828	0.0001†	0.001
Right coronary artery	0.058†	0.052	0.005†	0.947	0.469	0.494	0.039
Left coronary artery	0.098‡	0.87	0.059	0.070	0.829	0.044†	0.07
Left upper pulmonary vein	0.005†	0.763	0.006†	0.003‡	0.802	0.003†	0.001
Left lower pulmonary vein	0.001†	0.765	0.001†	0.001‡	0.986	0.001†	0.001
Right upper pulmonary vein	0.003†	0.63	0.012†	0.01‡	0.668	0.021†	0.003
Right lower pulmonary vein	0.01†	0.539	0.004†	0.0001‡	0.459	0.001†	0.001

†, the first method performs better; ‡, the second method performs better in the respective comparison. The P values in columns 2 through 6 represent the results of pairwise comparisons with the Wilcoxon Rank-Sum test between the two imaging methods specified in the header of each column. The P values in the 7th column correspond to the results of Kruskal-Wallis's test, which evaluates whether significant differences exist among all the imaging methods being compared. CS, compressed sense; DL, deep learning based (Adaptive-CS-Net) image reconstruction; MTC, magnetization transfer contrast; REACT, relaxation-enhanced angiography without contrast and triggering.

Figure 4 shows the difference between MTC-REACT images reconstructed using the CS and Adaptive CS-Net. Images reconstructed using the Adaptive-CS-Net reconstruction algorithm have fewer artifacts and noise than CS-reconstructed MTC-REACT images. Accordingly, the heart structures and pulmonary vessels are better defined. In the first subject, significant dephasing artifacts in the inferior vena cava (IVC) area can be seen in the CS reconstruction, yet the IVC is well-defined with the Adaptive-CS-Net reconstruction. In the second subject, some of the tiny pulmonary vessels are not clearly visible in the CS reconstruction; however, using Adaptive-CS-Net reconstruction, the vessels have a better definition. In the third subject, the myocardium and liver regions have significant noise when using CS reconstruction, making it difficult to identify some of the structures such as the papillary muscle, but with Adaptive-CS-Net reconstruction, they have better visualization. The clear delineation of the heart structures and other tiny vessels in the Adaptive-CS-Net reconstructed images compared to the CS reconstructed images demonstrates the advantage of using DL reconstruction algorithms for highly undersampled data.

Visual comparison of Adaptive-CS-Net reconstructed MTC-REACT and REACT images

The Adaptive-CS-Net reconstructed MTC-REACT images demonstrated qualitatively superior performance in capturing detailed vascular anatomy compared to the modified REACT sequence (*Figure 5*). All images were reconstructed using the Adaptive-CS-Net.

The MTC-REACT sequence enhances the visualization of intrathoracic extracardiac vessels, including small vessels (*Figure 5*). In the first subject, while a dephasing artifact is noticed in the right lower pulmonary vein with the REACT sequence, this artifact is not observed in the MTC-REACT sequence. In the second subject, whereas the MTC-REACT delineates the small branch of the pulmonary vein clearly, the modified REACT sequence was not able to visualize the small branch. In the third subject, the pulmonary arteries and veins appear blended in the REACT sequence but they are well-differentiated with MTC-REACT sequence. Lastly, in the fourth subject, the pulmonary vessels lack clear definition with the REACT sequence, whereas the MTC-REACT sequence provides better contrast and improved visualization of the branch pulmonary arteries.

Clinical examples of MTC-REACT images

Figure 6 presents a comparison between the Adaptive-CS-Net-reconstructed MTC-REACT and gadolinium-enhanced 3D bSSFP sequences in one patient.

The patient is a 7-year-old female with Ebstein's anomaly of the tricuspid valve, pulmonary atresia, and status post right bidirectional Glenn and Fontan palliation. The images highlight the Glenn and Fontan anastomosis as well as the

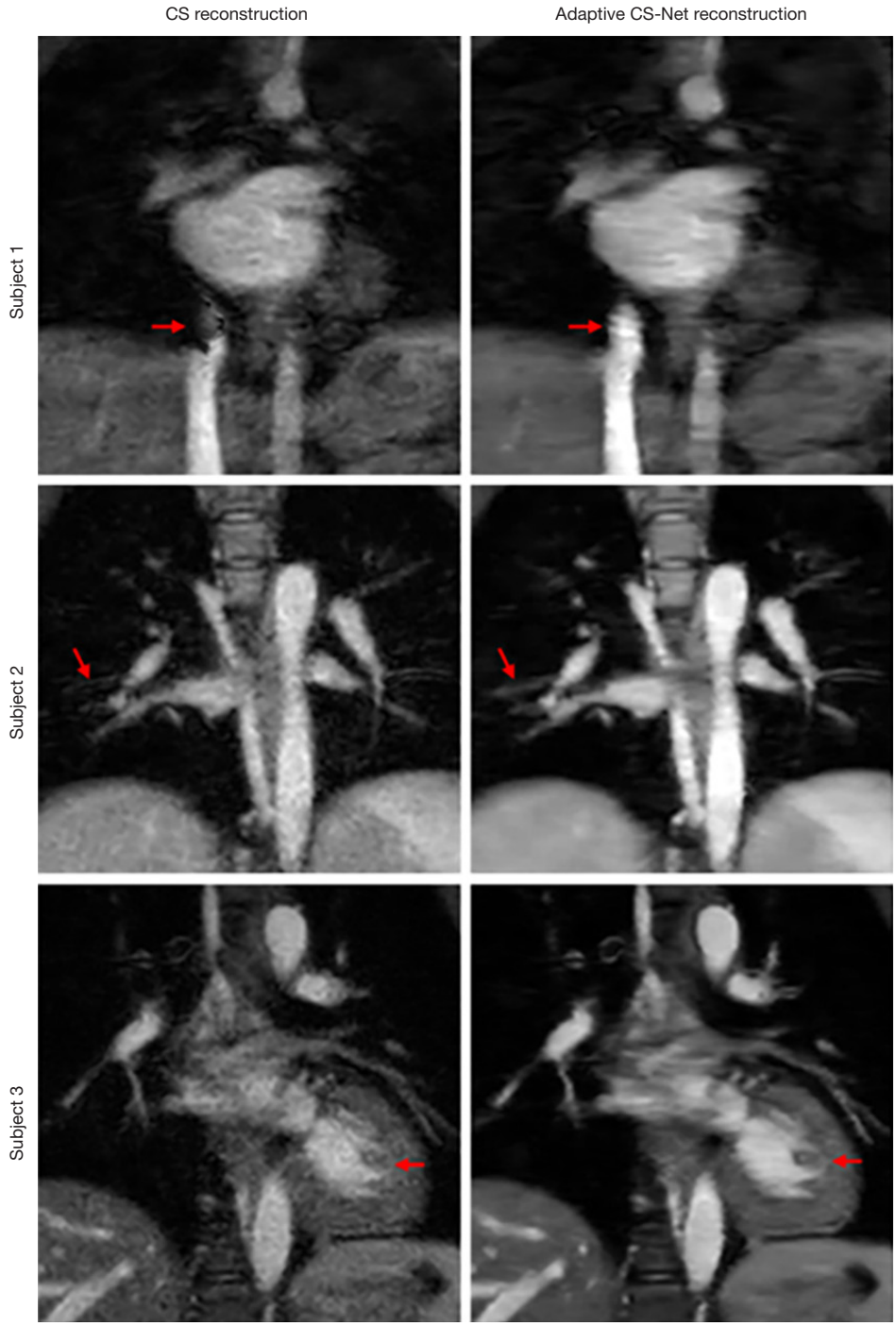

Figure 4 Visual comparison of CS reconstruction (left) and Adaptive-CS-Net reconstruction (right) of MTC-REACT data for three subjects. Red arrows highlight areas with clear differences between the two reconstruction methods. In the first subject, an artifact is observed in the inferior vena cava with CS reconstruction, which is noticeably reduced with Adaptive-CS-Net reconstruction. In the second subject, small branches of the right lower pulmonary artery are better defined with Adaptive-CS-Net reconstruction. For the third subject, significant noise is present in the myocardium and liver with CS reconstruction. In contrast, Adaptive-CS-Net reconstruction reduces the noise level and improves the differentiation of the endocardium-myocardium border, as well as the definition of the papillary muscle. CS, compressed sense; MTC-REACT, magnetization transfer contrast-relaxation-enhanced angiography without contrast and triggering.

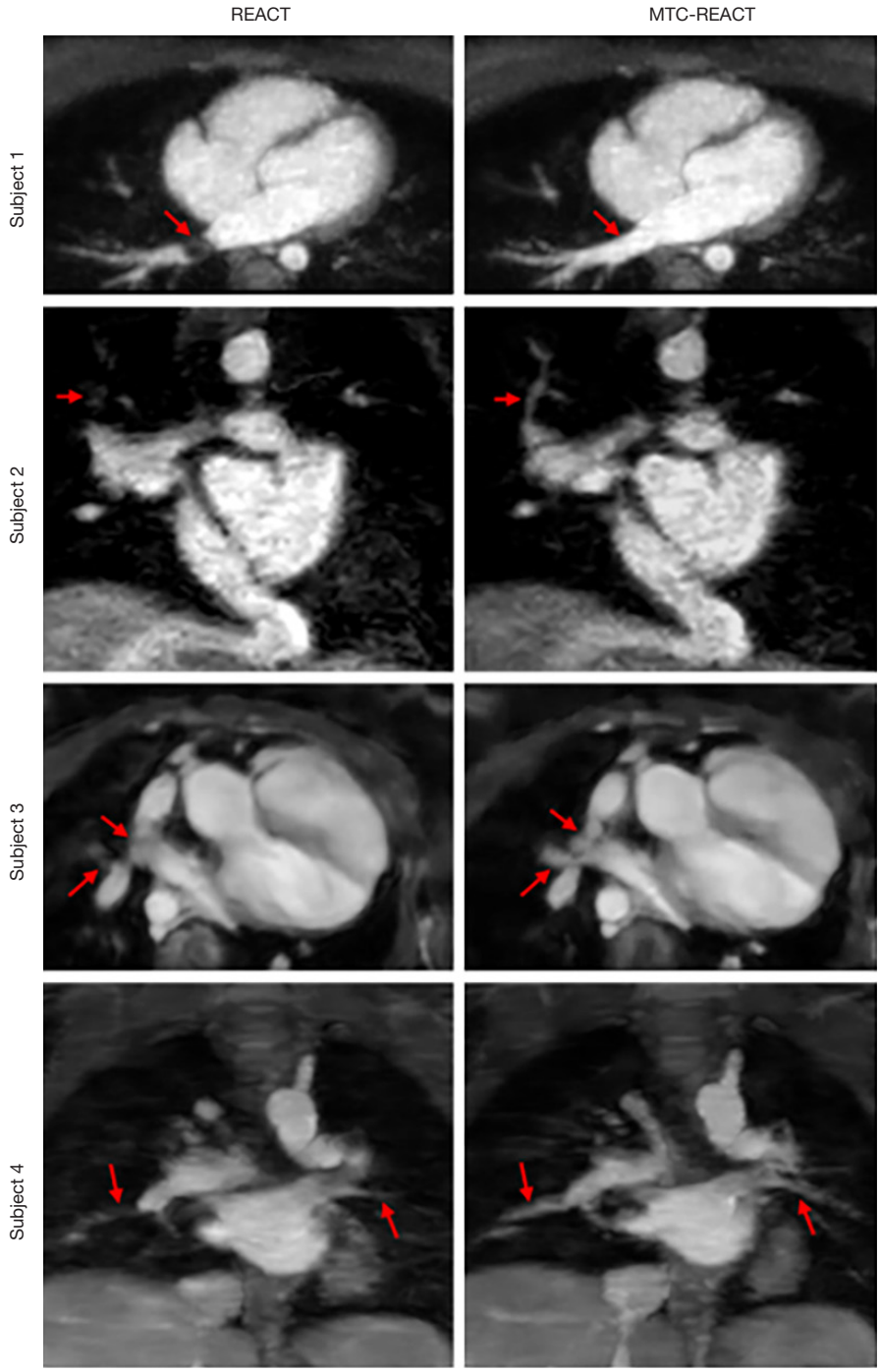

Figure 5 Visual comparison between the MTC-REACT sequence and the original REACT sequence. Images from four subjects comparing the original REACT (left) and MTC-REACT (right) for pulmonary veins, great vessels, and tiny pulmonary vessels were shown. In subject 1, the red arrows indicate that while the REACT image exhibits a dephasing artifact in the right lower pulmonary vein, MTC-REACT visualizes this vein. In subject 2, MTC-REACT successfully visualizes a small branch of the right upper pulmonary vein (right red arrow), which is not visible with the REACT sequence. In subject 3, MTC-REACT allows visualization of the right middle pulmonary vein (right red arrows), which is not visible in REACT images. In subject 4, MTC-REACT provides improved visualization of the right pulmonary artery and its lower lobe branch (left red arrow in the right image) as well as the left lower pulmonary vein (right red arrow in the right image) compared to REACT. MTC-REACT, magnetization transfer contrast-relaxation-enhanced angiography without contrast and triggering.

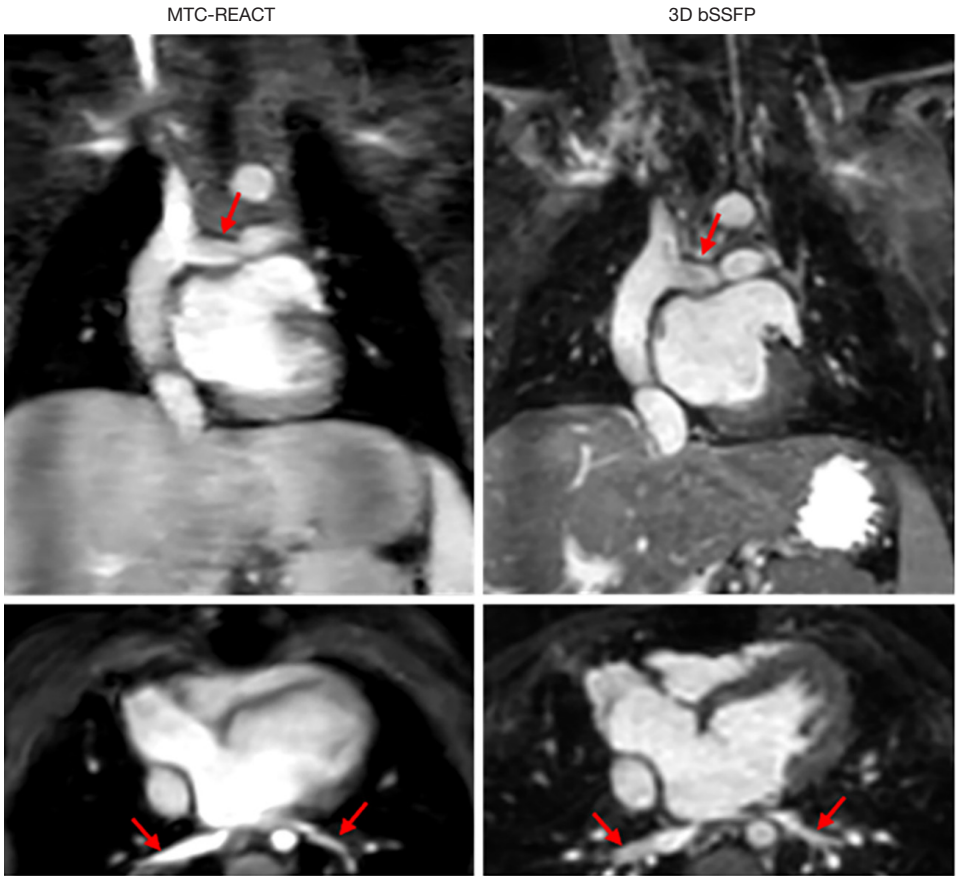

Figure 6 Illustration of the performance comparison between MTC-REACT and Gadolinium-enhanced 3D bSSFP sequence. Subject 2 is a 7-year-old female patient with Ebstein anomaly, critical pulmonary valve stenosis, and a history of Glenn and Fontan palliation. Both methods successfully image the Glenn and Fontan anastomosis, as well as the left pulmonary artery (red arrows, upper row). Additionally, both techniques visualize the left lower pulmonary vein (right arrows in each image of the lower row) and the right lower pulmonary vein (left arrows in each image of the lower row). This figure demonstrates that critical cardiac structures, including pulmonary arteries, pulmonary veins, and coronary arteries can be effectively captured using the MTC-REACT sequence without the need for contrast agents. The imaging quality achieved with MTC-REACT is comparable to that of the clinical contrast-enhanced 3D bSSFP sequence. 3D bSSFP, three-dimensional balanced steady-state free precession; MTC-REACT, magnetization transfer contrast-relaxation-enhanced angiography without contrast and triggering.

right and left lower pulmonary veins, captured by both the MTC-REACT sequence and the 3D bSSFP sequence, with red arrows pointing to the respective structures.

This figure demonstrates that the MTC-REACT sequence can achieve comparable anatomic detail to contrast-enhanced 3D bSSFP sequences, without requiring the use of a contrast agent.

Discussion

The preliminary findings of this study demonstrate the feasibility of a free-breathing MTC–REACT sequence combined with a DL-reconstruction framework for contrast-free imaging of intrathoracic vessels in patients with CHD and healthy volunteers. This study compared the MTC-REACT sequence with the modified REACT sequence, both reconstructed using DL-based methods, to evaluate the performance of the MTC pre-pulse. Additionally, it compared Adaptive CS-Net-reconstructed MTC-REACT with CS-reconstructed MTC-REACT to assess the performance of the DL reconstruction framework. The proposed framework offers several key advantages. First, the offline DL reconstruction framework for the MTC-REACT sequence significantly enhances

image quality compared to traditional online CS-based reconstruction methods. Second, the Adaptive-CS-Net reconstruction algorithm achieves a 10-fold acceleration in acquiring the MTC-REACT dataset, completing the process in approximately 2.5 minutes without compromising image quality. Finally, integrating an MTC pre-pulse with the REACT sequence (MTC-REACT) improves image quality, particularly for imaging pulmonary veins, compared to the REACT sequence. In terms of specific absorption rate (SAR), adding the MTC pre-pulse only increases 1% of the total SAR. The SAR for both REACT and MTC-REACT is less than 0.4 W/kg. These advantages underscore the potential of this framework for efficient and high-quality thoracic vessel imaging.

Currently, high spatial resolution, and cardiac- and respiratory-gated 3D bSSFP sequences are the standard for WH imaging (31). However, acquiring these sequences is time-consuming. CS and parallel imaging methods have been proposed to fasten image acquisition and improve patient comfort. Parallel imaging works by obtaining a reduced amount of k-space data with an array of receiver coils. These undersampled data can be acquired more quickly, but the undersampling is usually limited to 2 or 3 times to avoid aliased images (32). The CS approach requires a sparse image representation in a known transform domain, incoherent aliasing artifacts from k-space undersampling, and nonlinear reconstruction to enforce sparsity and data consistency (22). Despite the reconstruction being iterative and more computationally intensive than linear reconstruction methods, CS allows a significant reduction in scan time. However, for higher sampling factors, fixed sparsity assumptions in CS are often too restrictive and cause image quality deterioration (22). Deep-learning reconstruction techniques have recently been suggested as a potential to alleviate these limitations (33).

Adaptive-CS-Net is an adaptive intelligence method that leverages prior information, such as data consistency and known phase behavior, to enhance performance (27). Its iterative, learning-based reconstruction scheme is inspired by compressed sensing theory. The method employs deep neural networks to refine and correct prior reconstruction assumptions using the training data. In previous studies, Adaptive-CS-Net has been successfully applied to accelerate image acquisition and reconstruct various MR sequences. Fujima *et al.* have evaluated the utility of Adaptive-CS-Net image reconstruction by comparing it to conventional CS-based methods in fat-suppressed, contrast-enhanced 3D T1-weighted imaging for patients with head and neck disease, where high image quality and short scanning times are critical. The DL-based technique demonstrated clear superiority over CS-SENSE-based methods in imaging head and neck vessels (34). Another study showed that Adaptive-CS-Net reconstruction with a SENSE acceleration factor of 5 for retrospectively cardiac-gated 2D Cine bSSFP imaging can provide functional and volumetric indices equivalent to SENSE reconstruction with an acceleration factor of 2. This represents a 57% reduction in breath-hold time without compromising spatial or temporal resolution (35).

This study demonstrated that combining CS with a DL-based algorithm using Convolutional Neural Networks (Adaptive-CS-Net) achieved a 10-fold acceleration factor for MTC-REACT image reconstruction without loss of image quality compared to a CS-accelerated MTC-REACT reference scan. This rapid acquisition scheme reduced the scan time to slightly more than 2 minutes, offering consistent and predictable durations. The enhanced image quality might be attributed to reduced artifacts from cardiac motion and respiratory movement due to faster image acquisition.

Pulmonary veins, located near the lungs, are subject to resonance frequency shifts which can cause signal voids or banding artifacts in conventional non-contrast-enhanced T2-prepared SSFP sequences (5,36). These artifacts become more prominent at larger fields of view and higher magnetic field strengths like 3T. Recent innovations, including MT and inversion recovery preparation (3), interleaved T2-prep inversion recovery preparation (37), have shown promising results in improving image quality. However, REACT sequences provide robust and uniform background suppression by utilizing the dual-echo generalized Dixon method. This technique offers resistance to field inhomogeneity even when covering large fields of view or operating at higher field strengths, such as 3T. The REACT sequence has demonstrated superior pulmonary vein imaging compared to non-contrast-enhanced and contrast-enhanced 3D bSSFP sequences (19,21). MT pre-pulse further enhances pulmonary vein imaging by suppressing background tissue and myocardial signals while enhancing blood signal intensity (38). This additional preparation significantly contributes to better differentiation of the pulmonary veins from surrounding structures. Recent studies have also shown that MT and inversion recovery prepared 3D sequences improve pulmonary vein imaging in

patients with CHD (2,26,39). Similarly in this study, MTC-REACT significantly enhanced the SNR and CNR in the pulmonary veins compared to the REACT technique even when both methods used the same reconstruction method. However, this improvement was not reflected in the image quality scores, possibly due to the small cohort size.

Though this work shows preliminary results on the usage of the MTC-REACT technique in combination with the deep-learning reconstruction, it has some limitations. This is a single-center, small cohort study with mostly healthy volunteers. Further validation in large multicenter patient cohorts is needed. Due to the absence of a comparison between MTC-REACT sequence image quality and vessel measurements with the clinical standard 3D bSSFP images, the diagnostic capability of the MTC-REACT sequence cannot be fully validated. Furthermore, we only considered SNR, CNR and subjective image quality assessment for image quality comparison. This might not fully reflect the clinical scenarios. As this is a preliminary study and most of the participants are healthy volunteers, future work involving large patients population needs to be done to address the issue of diagnosis accuracy. In the future, patients with congenital and acquired heart diseases from different centers should be imaged with the MTC-REACT technique and 3D bSSFP sequence.

Conclusions

Our preliminary experience with MTC-REACT—a non-contrast-enhanced, free-breathing, WH imaging technique augmented by deep-learning-based reconstruction for 10-fold accelerated image acquisition—demonstrates its feasibility and promise in evaluating intrathoracic vascular structures, particularly pulmonary veins, across an anatomically diverse population. Integrating the MTC pre-pulse with the REACT sequence significantly enhances image quality and provides superior anatomical visualization of both small and large pulmonary arteries and veins within the thorax, surpassing the modified REACT sequence, irrespective of the deep-learning reconstruction method's impact.

Acknowledgments

During the preparation of this work, the authors used Grammarly (v1.2.85) to check the text for grammatical errors.

Footnote

Reporting Checklist: The authors have completed the TRIPOD + AI reporting checklist. Available at https://qims.amegroups.com/article/view/10.21037/qims-24-2199/rc

Funding: None.

Conflicts of Interest: All authors have completed the ICMJE uniform disclosure form (available at https://qims.amegroups.com/article/view/10.21037/qims-24-2199/coif). The authors have no conflicts of interest to declare.

Ethical Statement: The authors are accountable for all aspects of the work in ensuring that questions related to the accuracy or integrity of any part of the work are appropriately investigated and resolved. The study was conducted in accordance with the Declaration of Helsinki (as revised in 2013). The study was approved by the local institutional review board of the University of Texas Southwestern Medical Center (No. STU 032016009), and informed consent was obtained from all individual participants.

References

1. Greil G, Tandon AA, Silva Vieira M, Hussain T. 3D Whole Heart Imaging for Congenital Heart Disease. Front Pediatr 2017;5:36.
2. Rashid I, Ginami G, Nordio G, Fotaki A, Neji R, Alam H, Pushparajah K, Frigiola A, Valverde I, Botnar RM, Prieto C. Magnetization Transfer BOOST Noncontrast Angiography Improves Pulmonary Vein Imaging in Adults With Congenital Heart Disease. J Magn Reson Imaging 2023;57:521-31.
3. Uribe S, Tangchaoren T, Parish V, Wolf I, Razavi R, Greil G, Schaeffter T. Volumetric cardiac quantification by using 3D dual-phase whole-heart MR imaging. Radiology 2008;248:606-14.

4. Cukur T, Lee JH, Bangerter NK, Hargreaves BA, Nishimura DG. Non-contrast-enhanced flow-independent peripheral MR angiography with balanced SSFP. Magn Reson Med 2009;61:1533-9.
5. Hu P, Stoeck CT, Smink J, Peters DC, Ngo L, Goddu B, Kissinger KV, Goepfert LA, Chan J, Hauser TH, Rofsky NM, Manning WJ, Nezafat R. Noncontrast SSFP pulmonary vein magnetic resonance angiography: impact of off-resonance and flow. J Magn Reson Imaging 2010;32:1255-61.
6. Pilleul F, Merchant N. MRI of the pulmonary veins: comparison between 3D MR angiography and T1-weighted spin echo. J Comput Assist Tomogr 2000;24:683-7.
7. Zucker EJ. Cross-sectional imaging of congenital pulmonary artery anomalies. Int J Cardiovasc Imaging 2019;35:1535-48.
8. Rogosnitzky M, Branch S. Gadolinium-based contrast agent toxicity: a review of known and proposed mechanisms. Biometals 2016;29:365-76.
9. Chen Y, Guo H, Dong P, Li Y, Zhang Z, Mao N, Chu T, Sun Z, Wang F, Feng Z, Wang H, Ma H. Feasibility of 3.0 T balanced fast field echo non-contrast-enhanced whole-heart coronary magnetic resonance angiography. Cardiovasc Diagn Ther 2023;13:51-60.
10. Edelman RR, Koktzoglou I. Noncontrast MR angiography: An update. J Magn Reson Imaging 2019;49:355-73.
11. Kato Y, Ambale-Venkatesh B, Kassai Y, Kasuboski L, Schuijf J, Kapoor K, Caruthers S, Lima JAC. Non-contrast coronary magnetic resonance angiography: current frontiers and future horizons. MAGMA 2020;33:591-612.
12. Nakamura M, Kido T, Kido T, Watanabe K, Schmidt M, Forman C, Mochizuki T. Non-contrast compressed sensing whole-heart coronary magnetic resonance angiography at 3T: A comparison with conventional imaging. Eur J Radiol 2018;104:43-8.
13. Tan EJ, Zhang S, Tirukonda P, Chong LR. REACT - A novel flow-independent non-gated non-contrast MR angiography technique using magnetization-prepared 3D non-balanced dual-echo dixon method: Preliminary clinical experience. Eur J Radiol Open 2020;7:100238.
14. Yoneyama M, Zhang S, Hu HH, Chong LR, Bardo D, Miller JH, Toyonari N, Katahira K, Katsumata Y, Pokorney A, Ng CK, Kouwenhoven M, Van Cauteren M. Free-breathing non-contrast-enhanced flow-independent MR angiography using magnetization-prepared 3D non-balanced dual-echo Dixon method: A feasibility study at 3 Tesla. Magn Reson Imaging 2019;63:137-46.
15. Terwolbeck MN, Zhang S, Bode M, Yoneyama M, Kuhl CK, Kraemer NA. Relaxation-Enhanced Angiography without Contrast and Triggering (REACT) for pelvic MR venography in comparison to balanced gradient-echo and T2-weighted spin-echo techniques. Clin Imaging 2021;74:149-55.
16. Isaak A, Luetkens JA, Faron A, Endler C, Mesropyan N, Katemann C, Zhang S, Kupczyk P, Kuetting D, Attenberger U, Dabir D. Free-breathing non-contrast flow-independent cardiovascular magnetic resonance angiography using cardiac gated, magnetization-prepared 3D Dixon method: assessment of thoracic vasculature in congenital heart disease. J Cardiovasc Magn Reson 2021;23:91.
17. Isaak A, Mesropyan N, Hart C, Zhang S, Kravchenko D, Endler C, Katemann C, Weber O, Pieper CC, Kuetting D, Attenberger U, Dabir D, Luetkens JA. Non-contrast free-breathing 3D cardiovascular magnetic resonance angiography using REACT (relaxation-enhanced angiography without contrast) compared to contrast-enhanced steady-state magnetic resonance angiography in complex pediatric congenital heart disease at 3T. J Cardiovasc Magn Reson 2022;24:55.
18. Pennig L, Wagner A, Weiss K, Lennartz S, Huntgeburth M, Hickethier T, Maintz D, Naehle CP, Bunck AC, Doerner J. Comparison of a novel Compressed SENSE accelerated 3D modified relaxation-enhanced angiography without contrast and triggering with CE-MRA in imaging of the thoracic aorta. Int J Cardiovasc Imaging 2021;37:315-29.
19. Erdem S, Greil GF, Hussain MT, Zou Q. A novel non-contrast agent-enhanced 3D whole-heart magnetic resonance sequence for congenital heart disease patients: the REACT Study. Pediatr Radiol 2024;54:2199-209.
20. Gietzen C, Kaya K, Janssen JP, Gertz RJ, Terzis R, Huflage H, Grunz JP, Gietzen T, Pennig H, Celik E, Borggrefe J, Persigehl T, Kabbasch C, Weiss K, Goertz L, Pennig L. Highly compressed SENSE accelerated relaxation-enhanced angiography without contrast and triggering (REACT) for fast non-contrast enhanced magnetic resonance angiography of the neck: Clinical evaluation in patients with acute ischemic stroke at 3 tesla. Magn Reson Imaging 2024;112:27-37.
21. Pennig L, Wagner A, Weiss K, Lennartz S, Grunz JP, Maintz D, Laukamp KR, Hickethier T, Naehle CP, Bunck AC, Doerner J. Imaging of the pulmonary vasculature in congenital heart disease without gadolinium contrast: Intraindividual comparison of a novel Compressed SENSE

accelerated 3D modified REACT with 4D contrast-enhanced magnetic resonance angiography. J Cardiovasc Magn Reson 2020;22:8.
22. Lustig M, Donoho D, Pauly JM. Sparse MRI: The application of compressed sensing for rapid MR imaging. Magn Reson Med 2007;58:1182-95.
23. Singh D, Monga A, de Moura HL, Zhang X, Zibetti MVW, Regatte RR. Emerging Trends in Fast MRI Using Deep-Learning Reconstruction on Undersampled k-Space Data: A Systematic Review. Bioengineering (Basel) 2023;10:1012.
24. Hu BS, Conolly SM, Wright GA, Nishimura DG, Macovski A. Pulsed saturation transfer contrast. Magn Reson Med 1992;26:231-40.
25. Sled JG. Modelling and interpretation of magnetization transfer imaging in the brain. Neuroimage 2018;182:128-35.
26. Fotaki A, Pushparajah K, Hajhosseiny R, Schneider A, Alam H, Ferreira J, Neji R, Kunze KP, Frigiola A, Botnar RM, Prieto C. Free-breathing, Contrast Agent-free Whole-Heart MTC-BOOST Imaging: Single-Center Validation Study in Adult Congenital Heart Disease. Radiol Cardiothorac Imaging 2023;5:e220146.
27. Pezzotti N, de Weerdt E, Yousefi S, Elmahdy MS, van Gemert J, Schülke C, Doneva M, Nielsen T, Kastryulin S, Lelieveldt BPF, van Osch MJP, Staring M. Adaptive-CS-Net: FastMRI with Adaptive Intelligence. arXiv 2019. arXiv:1912.12259.
28. Zhang J, Ghanem B. ISTA-Net: Interpretable Optimization-Inspired Deep Network for Image Compressive Sensing. 2018 IEEE/CVF Conference on Computer Vision and Pattern Recognition. Salt Lake City, UT, USA: IEEE; 2018.
29. Lui D, Modhafar A, Haider MA, Wong A. Monte Carlo-based noise compensation in coil intensity corrected endorectal MRI. BMC Med Imaging 2015;15:43.
30. Chevallier O, Escande H, Ambarki K, Weiland E, Kuehn B, Guillen K, Manfredi S, Gehin S, Blanc J, Loffroy R. Single-Breath-Hold MRI-SPACE Cholangiopancreatography with Compressed Sensing versus Conventional Respiratory-Triggered MRI-SPACE Cholangiopancreatography at 3Tesla: Comparison of Image Quality and Diagnostic Confidence. Diagnostics (Basel) 2021;11:1886.
31. Fratz S, Chung T, Greil GF, Samyn MM, Taylor AM, Valsangiacomo Buechel ER, Yoo SJ, Powell AJ. Guidelines and protocols for cardiovascular magnetic resonance in children and adults with congenital heart disease: SCMR expert consensus group on congenital heart disease. J Cardiovasc Magn Reson 2013;15:51.
32. Deshmane A, Gulani V, Griswold MA, Seiberlich N. Parallel MR imaging. J Magn Reson Imaging 2012;36:55-72.
33. Bustin A, Fuin N, Botnar RM, Prieto C. From Compressed-Sensing to Artificial Intelligence-Based Cardiac MRI Reconstruction. Front Cardiovasc Med 2020;7:17.
34. Fujima N, Nakagawa J, Ikebe Y, Kameda H, Harada T, Shimizu Y, Tsushima N, Kano S, Homma A, Kwon J, Yoneyama M, Kudo K. Improved image quality in contrast-enhanced 3D-T1 weighted sequence by compressed sensing-based deep-learning reconstruction for the evaluation of head and neck. Magn Reson Imaging 2024;108:111-5.
35. Pednekar A, Kocaoglu M, Wang H, Tanimoto A, Tkach JA, Lang S, Taylor MD. Accelerated Cine Cardiac MRI Using Deep Learning-Based Reconstruction: A Systematic Evaluation. J Magn Reson Imaging 2024;60:640-50.
36. Scheffler K, Lehnhardt S. Principles and applications of balanced SSFP techniques. Eur Radiol 2003;13:2409-18.
37. Milotta G, Ginami G, Cruz G, Neji R, Prieto C, Botnar RM. Simultaneous 3D whole-heart bright-blood and black blood imaging for cardiovascular anatomy and wall assessment with interleaved T(2) prep-IR. Magn Reson Med 2019;82:312-25.
38. Li D, Paschal CB, Haacke EM, Adler LP. Coronary arteries: three-dimensional MR imaging with fat saturation and magnetization transfer contrast. Radiology 1993;187:401-6.
39. Fotaki A, Fuin N, Nordio G, Velasco Jimeno C, Qi H, Emmanuel Y, Pushparajah K, Botnar RM, Prieto C. Accelerating 3D MTC-BOOST in patients with congenital heart disease using a joint multi-scale variational neural network reconstruction. Magn Reson Imaging 2022;92:120-32.

Cite this article as: Erdem S, Jack A, Doctor P, Greil G, Hussain T, Zou Q. Feasibility of magnetization-transfer-contrast relaxation-enhanced angiography without contrast and triggering (REACT) imaging at 1.5 T combined with deep learning-based reconstruction for cardiovascular visualization. Quant Imaging Med Surg 2025;15(4):3222-3236. doi: 10.21037/qims-24-2199

